



1
2
3
4
5
6
7
8
9
10
11
12
13
14
15
16
17
18
19
20
21
22
23

Interpretation of Particle Number Size Distributions Measured across an Urban Area during the FASTER Campaign

**Roy M. Harrison^{1*†}, David C.S. Beddows¹
Mohammed S. Alam¹, Ajit Singh¹, James Brean¹,
Ruixin Xu¹, Simone Kotthaus² and Sue Grimmond²**

**¹Division of Environmental Health and Risk Management,
School of Geography, Earth and Environmental Sciences
University of Birmingham
Edgbaston, Birmingham B15 2TT
United Kingdom**

**²Department of Meteorology
University of Reading, Reading RG6 6BB
United Kingdom**

* To whom correspondence should be addressed.
Tele: +44 121 414 3494; Fax: +44 121 414 3709; Email: r.m.harrison@bham.ac.uk

†Also at: Department of Environmental Sciences / Center of Excellence in Environmental Studies, King Abdulaziz University, PO Box 80203, Jeddah, 21589, Saudi Arabia

24 **ABSTRACT**

25 Particle number size distributions have been measured simultaneously by Scanning Mobility
26 Particle Sizers (SMPS) at five sites in Central London for a one month campaign in January –
27 February 2017. These measurements were accompanied by condensation particle counters (CPC)
28 to measure total particle number count at four of the sites and aethalometers measuring Black
29 Carbon (BC) at five sites. The spatial distribution and inter-relationships of the particle size
30 distribution and SMPS total number counts with CPC total number counts and Black Carbon
31 measurements have been analysed in detail as well as variations in the size distributions. One site
32 (Marylebone Road) was in a heavily-trafficked street canyon, one site (Westminster University)
33 was on a rooftop adjacent to the Marylebone Road sampler, a further sampler was located at
34 Regent's University within a major park to the north of Marylebone Road. A fourth sampler was
35 located nearby at 160 m above ground level on the BT tower and a fifth sampler was located 4 km
36 to the west of the main sampling region at North Kensington. Consistent with earlier studies it was
37 found that the mode in the size distribution had shifted to smaller sizes at the Regent's University
38 (park) site, the mean particle shrinkage rate being 0.04 nm s^{-1} with slightly lower values at low wind
39 speeds and some larger values at higher wind speeds. There was evidence of complete evaporation
40 of the semi-volatile nucleation mode under certain conditions at the elevated BT Tower site.
41 Whereas SMPS total count and Black Carbon showed typical traffic-dominated diurnal profiles, the
42 CPC count data typically peaked during nighttime as did CPC/SMPS and CPC/BC ratios. This is
43 thought to be due to the presence of high concentrations of small particles (2.5 – 15 nm diameter)
44 probably arising from condensational growth from traffic emissions during the cooler nighttime
45 conditions. Such behaviour was most marked at the Regent's University and Westminster
46 University sites and less so at Marylebone Road, while at the elevated BT Tower site the ratio of
47 particle number (CPC) to Black Carbon peaked during the morning rush hour and not at nighttime,
48 unlike the other sites. An elevation in nucleation mode particles associated with winds from the



49 West and WSW sector was concluded to result from emissions from London Heathrow Airport,

50 despite a distance of 22 km from the Central London sites.

51

52 **1. INTRODUCTION**

53 The adverse health consequences of air polluted by particulate matter are now well recognised
54 (WHO, 2006). While the main focus has been on the public health impact of exposure to fine
55 particulate matter measured by mass ($PM_{2.5}$), there has also been concern over the possible
56 contribution of ultrafine particles of less than 100 nm diameter to adverse health outcomes. While
57 such particles contribute little to the total mass of particles in the atmosphere, they dominate particle
58 number (Harrison et al., 2000) and authoritative reviews have concluded that although evidence is
59 currently highly incomplete, they may contribute to the toxic hazard associated with ambient
60 particulate matter (HEI, 2013; WHO, 2013). There have also been suggestions that particle surface
61 area plays a major role in health impacts and this resides largely in the accumulation mode which is
62 typically centred around 100-200 nm diameter (Harrison et al., 2000). Consequently, there is a
63 strong interest from a health perspective in sub-micrometre particles and there are many reports of
64 their concentrations and size distributions within the atmosphere.

65
66 In addition to concerns over human health, there are other reasons for the study of the size
67 distribution of airborne particles. Not only does this strongly influence their location and efficiency
68 of deposition in the human lung, the particle size distribution can also be a strong indicator of
69 particle source, with there being some clear differences between the modal diameter of particles
70 arising from different sources (Vu et al., 2015a). The clearest distinction is between particles
71 arising from combustion and other high temperature sources, which tend to be predominantly very
72 small, and particles generated by attrition processes which are typically far more coarse. However,
73 even within the particles generated from combustion and other high temperature sources, there may
74 well be different modal diameters associated with different sources or even multiple modes
75 associated with an individual source (Vu et al., 2015a). For example, exhaust emissions from diesel
76 engines typically comprise both a nucleation mode and an overlapping Aitken mode, reflecting in
77 the former case particles comprised mainly of condensed lubricating oil formed after the



78 combustion process, and in the latter case, solid carbonaceous particles formed within the
79 combustion process (Shi and Harrison, 1999; Alam et al., 2016).

80
81 After their emission, particle size distributions are also liable to change through dynamic processes.
82 These include evaporation which causes particles to shrink without changing the overall number,
83 condensation which causes particles to grow without a change in total number, coagulation which
84 also causes growth but reduces the total particle number, and deposition which causes a reduction in
85 number and is a strong function of the particle size.

86
87 Within this study, particle number size distributions were measured simultaneously by electrical
88 mobility spectrometers at five separate sites across London and the size distributions are compared
89 with a view to gaining a better understanding of the sources and processes affecting particles in the
90 urban atmosphere.

91

92 **2. EXPERIMENTAL**

93
94 Data were collected from 27 January 2017 to 16 February 2017 as part of the second campaign of
95 the FASTER project. Data recovery was high at all sites except Westminster University, where
96 good SMPS data were collected on only three days, January 30 and 31 and February 1, 2017.

97

98 **2.1 Sampling Sites**

99 Data were collected at five sampling sites in total, three of which were established specifically for
100 the FASTER campaign, Westminster University, Regent's University and BT Tower. The other
101 two sites (London Marylebone Road and London North Kensington) collect data as part of the
102 national Automatic Urban and Rural Network. The site locations (seen in Figure 1) and
103 characteristics are as follows:



- 104 • *Marylebone Road.* Air sampling equipment is housed in a large kerbside cabin on the sidewalk
105 of a busy central London street canyon with an inlet approximately 2.5 m above ground-level
106 (agl). The adjacent six-lane highway carries around 80,000 vehicles per day. The highway is
107 relatively straight and runs almost due east-west (angle 80° from north). The buildings on
108 either side of the highway are around six storeys in height giving a street canyon aspect ratio of
109 approximately 1:1.
- 110 • *Westminster University.* Air sampling instruments were located on the roof of the Westminster
111 University building, almost directly above the Marylebone Road air sampling site on the
112 southern side of the street. The instruments were housed in a temporary enclosure located
113 approximately 26 m above street level and 4.5 m from the front edge of the roof where it
114 overlooks the road, and with an inlet 1.5 above the roof.
- 115 • *Regent's University.* A temporary enclosure for the instruments was located on the roof of
116 Regent's University which is an isolated building within Regent's Park due north (i.e. 360°) of
117 the Marylebone Road and Westminster University sites. The only highway lying between
118 Marylebone Road and the Regent's College site is a lightly trafficked road within Regent's
119 Park. The distance between the Westminster University and Regent's University sites is
120 estimated at 380 m. The instruments were located 16 m agl and 1 m from the edge of the roof.
- 121 • *London North Kensington.* Instruments were sited in a permanent cabin located within the
122 grounds of a high school in a lightly trafficked suburban area of central London, with an inlet
123 approximately 2.5 m agl. The air pollution climate at this site, often taken as representative of
124 the background air quality within central London, has been characterised in detail by Bigi and
125 Harrison (2010).
- 126 • *BT Tower.* Instruments were sited on level T35 at approximately 160 m agl on a narrow tower
127 which rises well above the surrounding buildings on a quietly trafficked street approximately
128 380 m to the south of Marylebone Road. The site was used extensively in the REPARTEE
129 experiment (Harrison et al., 2012a).



130 2.2 Sampling Instruments

131 The instruments (Table 1) were operated according to Wiedensohler et al. (2012) guidelines and
132 calibrated and intercompared both before and after the sampling campaign. Small correction factors
133 (< 5%) were applied to CPC (condensation particle counter) data as a result of the intercomparison.
134 SMPS (scanning mobility particle sizers) data were analysed using the AIM9 and AIM10 software
135 provided by TSI as appropriate to the instrument. The national network sites (Marylebone Road
136 and North Kensington) are fitted with diffusion dryers according to EUSAAR/ACTRIS protocols
137 (Wiedensohler et al., 2012), but the other sites were not. The particle size ranges measured were
138 14.9-615.3 nm at Westminster University, Regent's University and BT Tower, 16.55-604.3 nm at
139 Marylebone Road and North Kensington, and a further system with a short DMA (differential
140 mobility analyses) gave 4.96-145.9 nm at Regent's University.

141

142 It was not possible to use identical SMPS systems at each site. The variants used are shown in
143 Table 1. We expect little difference between the long column classifiers (TSI 3081) used at all sites
144 but with different platforms (TSI 3080 and TSI 3082) and CPCs (TSI 3775 and 3776). Differences
145 are expected to be minimal as platform-specific software was used to invert the data and both the
146 CPC are butanol-based, with only slightly different lower cut-points which were well outside of the
147 range of measured particles. At the Regent's University site, both a long DMA (3081) and short
148 column DMA (3085) were utilised and the data were merged to give a single continuous size
149 distribution from 6 nm to 650 nm. A possible cause of divergence is the fact that two of the sites
150 (Marylebone Road and North Kensington) used diffusion dryers according to the EUSAAR/
151 ACTRIS Protocol. The dryers were tested when installed and showed very low particle losses (less
152 than 5%) and no significant change to particle size distributions (NPL, 2010). The dryer may,
153 however, affect the particle size distribution due to the hygroscopicity of certain kinds of particles.
154 Vu et al. (2015b) reviewed hygroscopic growth factors for submicron aerosols from different
155 sources. Their data are difficult to extrapolate to this study as measurements of hygroscopic growth



156 are typically made at very high relative humidities, normally around 90%. Even at 99.5% relative
157 humidity, the growth of particles of less than 100 nm sampled from the atmosphere is relatively low
158 (Vu et al., 2015b). Consequently, a reduction in humidity from 88% typical of the campaign to the
159 values of 30-40% achieved in the dryer would be expected to have only a small effect on particle
160 sizes especially as fresh traffic-generated particles which comprise a large proportion of the sub-
161 micrometre particulate matter in the urban atmosphere are hydrophobic and therefore undergo zero
162 or very limited growth in humid atmospheres.

163

164 **2.3 Weather Conditions During the Campaign**

165 Wind speed and direction data were taken from Heathrow Airport to the west of London to reflect
166 the synoptic flow minimally affected by local building effects. At the start of the campaign (27
167 January 2017) the wind direction was easterly and moved to southerly by January 29th, briefly
168 passing through northerly before returning to a southerly circulation between January 31 and
169 February 3rd. During this time, wind speeds were typically around 4 m s^{-1} and temperatures mild
170 for the time of the year (mostly 6-10 °C). From February 4th to 8th there was a period of lower
171 wind speeds ($1\text{-}4 \text{ m s}^{-1}$) with variable wind directions and low nocturnal minima temperatures
172 (down to 1°C). From February 8 – 12th, a period of northerly winds (speeds of $3\text{-}5 \text{ m s}^{-1}$) and lower
173 temperatures (1-3°C) without appreciable diurnal variation occurred. After February 12th, the
174 winds came from the east moving to south-westerly by February 17th, with wind speeds variable
175 (between 0 and 6 m s^{-1}) and temperatures steadily rising to daily maxima of 12°C.

176

177 The mixed layer heights (MLH) were determined from Vaisala CL31 ceilometer data collected at
178 the Marylebone Road site (Figure 1, Table 1). The observed 15 s (10 m gates) aerosol attenuated
179 backscatter profiles were pre-processed (Kotthaus et al., 2016) prior to using the CABAM
180 algorithm (Kotthaus and Grimmond, 2018) to determine 15 min intervals MLH. The multiple
181 aerosol layers (e.g. nocturnal residual layers) in the atmosphere are detected (Kotthaus and



182 Grimmond, 2018; Kotthaus et al., 2018). Here the lowest detected layer is analysed. At times the
183 MLH cannot be detected (e.g. during rain or very weak gradients in attenuated backscatter), but a
184 residual layer might still be indicated. The ceilometer detects periods of precipitation, including
185 events that may not be recorded by ground-based stations (e.g. insufficient to trigger a tipping
186 bucket rain-gauge).

187

188 During the campaign the observed MLH varied from a daily minimum of 45 m agl to a daily
189 maximum of 1312 m agl with an overall 15 min average (median) of 421 (382) m agl. The daily
190 average (median) maximum MLH was 777 (695) and minimum was 194 (197) m agl. The daily
191 range and the amount of data available per day are shown in Figure S10.

192

193 **2.4 Modal Analysis of Size Distributions**

194 Modes were fitted to the 15 min data obtained at Marylebone Road, Regent's and Westminster
195 Universities using curve fitting and data analysis software "Fityk (version 1.3.1)" developed by
196 Wojdyr (2010). In the present analysis, a standard peak function (equation 1) was used to
197 disaggregate the size distributions into lognormal modes:

$$P_i = A_i \cdot \exp\left[-\left(\frac{\ln(D/c_i)}{W_i}\right)^2\right] \quad (1)$$

198 By fitting linear a combination of n peaks ($P_1 + P_2 + \dots + P_i + \dots + P_n$) to the number size
199 distributions, the following information was calculated: 1) amplitude A_i and location of $dN/d\log D$ at
200 the mode of the distribution c_i , 2) area under the curve (nm cm^{-3}), and 3) width of the lognormal
201 curve W_i .

202

203

204

205



206 **3. RESULTS AND DISCUSSION**

207 **3.1 Particle Size Distributions**

208 A time series of total particle number concentrations from the SMPS instruments appears in Figure
209 2. A strong diurnal variation is seen at all sites and is exemplified by the average daily variation
210 shown in Figure 3.

211

212 The data stratified by LHR wind direction (Figure 4) were used to perform the modal analysis. The
213 log normal modes fit to the size distribution were used to provide insights into the separate modes
214 contributing to a measured size distribution. Although most measurements could be fit with three
215 separate modes some distributions were best fit with only two modes. An example of a three mode
216 fit of a size distribution from North Kensington appears in the data for the 270° wind sector at this
217 site (Figure 5). It may be seen that using three modes gives a very good overall fit to the data. The
218 details of the modes fitted and their relative magnitude and breadth appear in Table S1.

219

220 The Marylebone Road sampling site is located in a heavily trafficked (approx. 80,000 vehicles per
221 day) street canyon. The canyon is aligned almost east-west and the sampling site is at kerbside on
222 the southern side of the street. The canyon has a height to width ratio of ~1 consequently we expect
223 skimming flow when flow is perpendicular, with one or more vortices established in the canyon
224 (Oke et al. 2017). When there is one vortex, the sampler is exposed to freshly emitted traffic
225 contaminants when the wind above the canyon is from the south (Figure 6). Particle number
226 concentration on Marylebone Road is highest for the 225° and 270° wind sectors (Figure 4a) when
227 traffic-generated pollutants are carried efficiently to the sampler. When winds have a northerly
228 component such as those for 0° and 45° in Figure 4a, the air reaching the sampler is typical of
229 background air from north London and peak concentrations fall by a substantial margin. The
230 particle size data from Marylebone Road (Table S1) show no strong effect of wind direction on the
231 modal diameter for the first fitted mode in the distribution. The average diameter for the 180 and



232 225° wind sectors are 21.4 nm while for the 0 and 45° sectors they are 22.9 nm. The second and
233 third mode in the distribution are far more sensitive to wind direction, with the southerly traffic-
234 dominated wind directions showing modes at around 32 and 76 nm as opposed to 56 nm and 263
235 nm for the northerly mode data. The former values compare well with modes in the number
236 distribution of around 20 nm and 50 nm previously attributed to the nucleation mode and Aitken
237 mode particles respectively from engine exhaust when sampled at Marylebone Road, with data
238 analysed by Positive Matrix Factorization (Harrison et al., 2011).

239

240 The Westminster University sampling site is 26 m higher and slightly displaced (~8 m) horizontally
241 from the Marylebone Road air sampling station. The observations at roof level are influenced by
242 the flow separation over the roof, if the air is entering or exiting the canyon, and the background
243 concentrations. The particle size data (Table S1) indicate a nucleation mode very similar in size to
244 that observed within the street canyon at the Marylebone Road site. Concentrations are elevated for
245 the 135 and 180° wind bearings suggesting that enhanced concentrations occurring within the
246 canyon on southerly winds are also elevated at the Westminster University sampler but the dataset
247 is very small and hence not included in Figure 4. The second mode appears to be broadly similar in
248 size to that at Marylebone Road and falls within the range of modal diameters measured at
249 Marylebone Road. Similarly, the third mode falls within the rather variable range also seen at
250 Marylebone Road.

251

252 The North Kensington site is widely taken as representative of the background air pollution climate
253 in central London (Bigi and Harrison, 2010; Bohnenstengel et al., 2015). At this site, the size of the
254 first mode in the size distributions is remarkably constant at 22-26 nm which is slightly larger than
255 that observed at Marylebone Road. The second mode is also less variable than at most other sites
256 and broadly within the range of the second mode sizes at Marylebone Road (see Table S1). The
257 third mode is highly variable in size with wind direction but again broadly comparable to the data



258 from Marylebone Road. The Beddows et al. (2015) Positive Matrix Factorization of particle
259 number size distributions data from this site identified four factors contributing to the particle
260 number size distributions: a secondary component accounting for 4.4% of particle number with a
261 mode at around 250 nm, an urban background factor (43% of particle number) peaking at around 50
262 nm, a traffic component (44.8% of particle number) peaking at around 30 nm and a regional
263 nucleation component (7.8% of particle number) peaking at 20 nm. The regional nucleation
264 component showed a strong seasonality with greatest prevalence in the summer months and is
265 thought unlikely to have contributed significantly during the period of this campaign.
266 Consequently, the first mode observed in our current study is very comparable to the traffic mode
267 observed by Beddows et al. (2015), and the second mode corresponds strongly to the urban
268 background factor identified by Beddows et al. (2015) who associated this factor with aged traffic
269 emissions and wood smoke, the latter of which is unlikely to have influenced the size distribution at
270 Marylebone Road significantly.

271

272 3.2 Particle Shrinkage

273 Previous London work has shown the tendency of nucleation mode traffic-generated particles
274 sampled within Regent's Park to have shrunk by evaporation at rates of on average 0.13 nm s^{-1}
275 (Harrison et al., 2016) while particles in the regional atmosphere typically undergo condensational
276 growth at a rate of about $0.6\text{-}0.9 \text{ nm h}^{-1}$ (Beddows et al., 2014). This reflects an initial local rapid
277 loss of more volatile hydrocarbons, followed by a subsequent slower condensation of low volatility
278 species formed by atmospheric oxidation in the regional atmosphere.

279

280 Under southerly flows the Regent's University site is downwind of Marylebone Road (Fig. 1). The
281 modal diameters measured at Regent's University in the nucleation mode (Table S1) are clearly
282 indicative of a shrinkage of particle diameter for the wind sectors 180° , 225° and 270° ,
283 corresponding to air having passed over Marylebone Road. These data show that the nucleation



284 mode is shrinking from a diameter in the range of 21-24 nm at Marylebone Road, and 22-24 nm at
285 Westminster University to a diameter of 14, 9 or 12 nm at the Regent's University site. In this case,
286 particle shrinkage seems to be limited to those three wind sectors, with possibly some shrinkage in
287 the 45° wind sector, but particles in other wind sectors retain broadly similar diameters to those
288 measured at Marylebone Road and Westminster University. The second particle mode and third
289 particle mode (where identifiable) at Regent's University are broadly similar and considerably
290 larger than those measured at Marylebone Road or in the limited dataset at Westminster University.

291

292 In our earlier studies of the evolution of particle sizes between Marylebone Road and Regent's Park
293 (Harrison et al., 2016), the nucleation mode in the Marylebone Road size distributions lay between
294 20-24 nm (i.e. very similar to this study). In Regent's Park this had reduced to within the range of
295 6-11 nm with the largest sizes measured in the 0° wind sector and the smallest in the 180° wind
296 sector. The current data show a similar general pattern, although the extent of size reduction is
297 smaller. The travel distance to the Regent's University site is shorter, hence accounting in part for
298 less shrinkage, but the overall shrinkage rate in the current study (0.04 nm s^{-1}) was smaller than
299 previously (0.13 nm s^{-1}) (Harrison et al, 2016). This is probably explained by two factors. Firstly,
300 with warmer mean air temperatures (12-18°C) evaporation would be enhanced, and secondly, as the
301 site used for collection of the data described in the Harrison et al. (2016) study was in the centre of
302 the park and further from any major highways than the Regent's University site, it may have
303 experienced lower vapour concentrations. Consequently, the two datasets appear highly consistent
304 with one another.

305

306 Previous BT Tower site observations have reported loss of < 20 nm particles (Dall'Osto et al.
307 2011). This loss was greatest when atmospheric turbulence levels were lowest and hence the time
308 for ground to sampling height (160 m) transport greatest. That analysis is not repeated in this study.
309 However, the nucleation mode size (Table S1) has grown slightly from the sizes measured at



310 Marylebone Road for the nucleation mode. It is notable that unlike the earlier results, the amplitude
311 of this mode at the BT Tower was substantial and slightly larger than that observed at the ground-
312 level background North Kensington site suggesting that there was generally good coupling between
313 ground-level and the Tower site. It is notable that the first mode diameter with greatest amplitude
314 was for the 270° sector (Figure 4d); this is discussed later. The particle size distribution associated
315 with the 225° wind sector had only one mode at 40 nm suggestive of the second solid particle mode
316 with complete evaporation of the semi-volatile nucleation mode.

317

318 Earlier studies have shown that particle number concentrations (< 100 nm) in a street canyon
319 (Olivares et al., 2007) and urban air (Hussein et al., 2006) increase with reducing temperature. This
320 is consistent with the semi-volatility of nucleation mode particles from road traffic (Harrison et al.,
321 2016), and consequently it would be expected that the particle size distribution as well as the
322 number concentration would be affected by ambient temperature. To investigate this, the size
323 distributions collected in the lowest quartile of air temperatures (1.1 to 3.8°C) were compared with
324 those in the highest quartile of temperature (9.1 to 11.8°C). This showed generally higher
325 concentrations associated with the higher temperatures, and a clearer nucleation mode at higher
326 temperatures, at all sites, and most notably at Marylebone Road. Such behaviour is contrary to
327 expectations, as greater evaporative losses would be expected at higher temperatures, reducing the
328 magnitude of the plot, or shifting the mode to smaller sizes. To understand this effect more clearly,
329 wind directions with the coldest and hottest quartiles of temperature are analysed. The coldest
330 periods all occurred during northerly flows (270 to 90°) and >85% of highest quartile of
331 temperatures occur during southerlies (90 to 270°). The behaviour, especially at Marylebone Road
332 and Regent's University therefore appears to be determined predominantly by synoptic wind
333 conditions. For Marylebone Road, the street canyon flow (Figure 6) is the dominant influence and
334 at Regent's University the traffic sources are most proximate with southerly flows.

335



336 3.3 Particle Number Concentration (CPC) Data

337 Average diurnal variations of total particle number count derived from the Condensation Particle
338 Counters produced using the Openair Software Package (Carslaw and Ropkins, 2012) appear in
339 Figure S1. Perhaps surprisingly, at both Marylebone Road and Westminster University, these show
340 a peak occurs between midnight and 6 am before reducing and then rising to a second peak in the
341 afternoon. CPC concentrations at these sites far exceed those at Regent's University and the BT
342 Tower, whereas integrated counts from the SMPS instruments were considerably smaller and
343 showed a diurnal variation broadly similar to that expected for road traffic emissions (Figure 3).
344 While it is quite normal for the CPC to give a higher count than the SMPS since it measures over a
345 wider size range and may have lower internal losses (although the SMPS data analysis software
346 corrects for internal losses), the ratio of CPC to SMPS is typically around two, but this value was
347 significantly exceeded episodically, especially at Westminster University (Figure S2). The overall
348 pattern of CPC to SMPS ratios (Figure 7) shows that some of the highest ratios were at Regent's
349 University with two individual occasions exceeding 13. Some high peak values were observed at
350 Westminster University during the short SMPS time series. Wood burning is recognised as an
351 influential source of particles in London (Harrison et al, 2012b; Crilley et al., 2015), and has a
352 diurnal profile with higher concentrations typically at night. During the ClearfLo winter campaign
353 the BT Tower was influenced substantially by wood smoke irrespective of boundary layer depth
354 (Crilley et al, 2015). Since the BT Tower site was predominantly within the mixed layer during the
355 2017 campaign (Figure S10) and the CPC/SMPS average ratios at the Tower show little nocturnal
356 elevation, we consider it unlikely that wood smoke explains our observations. Furthermore, particle
357 size distributions associated with biomass burning are typically larger than those from road traffic,
358 and outside of the sub-15 nm size range (Vu et al., 2015a).

359

360 To evaluate this phenomenon more closely, the Black Carbon data were examined. These are
361 typically taken as a good tracer of diesel exhaust which is expected to be the main source of the



362 particle number count. The diurnal variation in Black Carbon (Figure S3) conformed reasonably
363 well to that expected for a traffic-generated pollutant with Marylebone Road concentrations far
364 exceeding those at the other sites and showing a typical traffic-associated pattern. Particle number
365 (derived from the CPC) to Black Carbon ratio (Figure S4) shows huge diurnal variability similar to
366 that seen in the ratio of particle number count from the CPC to that derived from the SMPS. We
367 infer from this behaviour that a large number of particles smaller than the lower limit of the SMPS
368 and above the lower limit of the CPC (i.e. 2.5-14.9 nm for the 3776 instrument at Westminster
369 University and Regent's University; 4-14.9 nm for 3775 instrument at BT Tower; and 3-16.55 nm
370 for 3025 instrument at Marylebone Road) were present in the atmosphere. Both the mean ratio of
371 CPC to SMPS (Figure S2) and CPC to Black Carbon (Figure S5) have ratios that are greatest in the
372 early morning (midnight to 6 am). This is unexpected for the CPC/SMPS ratio, as the contribution
373 of traffic relative to regional aerosol is expected to be least and the coarser regional aerosol contains
374 few particles in the size range below the lower limit of the SMPS instrument. Similarly, for the
375 Black Carbon data, one would expect that if traffic is the main source of particles measured by the
376 CPC, the latter would show a diurnal fluctuation like that of Black Carbon, which in London arises
377 mostly from traffic emissions. Consequently, it seems likely that nucleation processes favoured by
378 the cooler temperatures and lower condensation sink in the early hours of the morning are creating
379 large numbers of particles in the range of 2.5-15 nm mobility diameter. These are forming as air
380 moves away from the traffic source and hence are greatest at the rooftop Westminster University
381 site and have diminished to some extent by coagulation or re-evaporation by the time they reach the
382 Regent's University site which still shows a marked elevation in particle number to Black
383 Carbon ratio in the earlier hours of the morning compared to the Marylebone Road site.

384

385 Such behaviour is somewhat unexpected and a review of papers in which vertical gradients in
386 particle number count have been measured above roadside sites showed no earlier evidence of such
387 behaviour (Lingard et al., 2006; Agus et al., 2007; Nikolova et al., 2011; Ketznel et al., 2003;



388 Longley et al., 2003; Kumar et al., 2008a,b; Kumar et al., 2009; Li et al., 2007; Vakeva et al.,
389 1999; Zhu et al., 2002; Wehner et al., 2002). However, evidence is seen in some of Villa et al.'s
390 (2017) observations, particle number count increased with height up to around 10 m above a multi-
391 lane highway. The authors reported this unexpected pattern for some ascents/descents and
392 attributed it to exhaust tubes of heavy duty trucks tending to project vertically upwards and to be
393 located at a height of several metres above ground. They suggest this is not the case in urban
394 canyons.

395

396 Another possibility arises from the report of Rönkkö et al. (2017) that large numbers of sub-4 nm
397 particles are observed in the exhaust of some diesel engines and the observation by Nosko et al.
398 (2017) of substantial numbers of similarly sized particles amongst emissions from brake wear.
399 Kontkanen et al. (2017) reported observations of sub-3 nm particles from many sites, the highest
400 concentrations being in urban locations. The diurnal and regional variations did not relate clearly to
401 photochemistry and it was concluded that sub-3 nm particle concentrations are affected by
402 anthropogenic sources of precursor vapours. The correlation of sub-3 nm particle concentrations in
403 Helsinki with nitrogen oxides suggested a link with traffic emissions. Shi et al. (2001) measured
404 particles of >9.5 nm by SMPS, >7 nm by CPC and >3 nm by ultrafine CPC, finding large numbers
405 of particles in urban air in the ranges 3-7 nm and 3-9.5 nm by differences of counts. Ratios of CPC
406 (>3 nm):SMPS (>9.5 nm) were highly variable, but typically around 4. Clear links to road traffic
407 were seen, with drive-by experiments showing large numbers of particles in the 3-7 nm range in the
408 exhausts of both diesel and gasoline vehicles (Shi et al., 2001). Nanoparticles were also produced
409 in the plume downwind of a stationary combustion source (Shi et al., 2001). Herner et al. (2011)
410 measured the size distribution of particles emitted from vehicles equipped with diesel particle
411 filters, and with diesel filters and selective catalytic reduction. The dominant mode in the size
412 distribution was at 10 nm diameter and comprised particles with a high fraction of sulphate. In
413 highway and roadside measurements in Helsinki, Enroth et al. (2016) measured particle size



414 distributions with a dominant mode at 10 nm diameter. Such particles would be largely below the
415 lower threshold for counting by the SMPS but not the CPC. It is plausible that during the cooler
416 hours of the night a tail of <2.5 nm particles might be subject to condensational growth if the co-
417 emitted vapour were to be supersaturated in the atmosphere within the street canyon. The
418 dominance of a 10 nm mode in the size distribution would appear to be the most plausible
419 explanation for the high number concentration of particles observed at the Westminster University
420 rooftop location and the apparent transport of a substantial proportion of such particles to the
421 Regent's University measurement site. While this can explain the typically high CPC/SMPS ratios
422 observed, it does not explain their diurnal variation. This appears to require growth of sub-2.5 nm
423 particles into the range measured by CPC in the cooler, more humid nocturnal conditions. Rönkkö
424 et al. (2006) and Schneider et al. (2005) studied the formation of mechanisms and composition of
425 diesel exhaust nucleation particles in the laboratory and during car chasing. They conclude that
426 formation of nucleation mode particles depends upon formation of sulphate nuclei upon which
427 hydrocarbons condense, consistent with earlier studies of Shi and Harrison (1999) and Shi et al.
428 (2000) conducted in our laboratory. Factors favouring nucleation mode particle formation were
429 found to be low temperature and high humidities, consistent with field measurements made on
430 Marylebone Road (Charron and Harrison, 2003). Both factors prevail at nighttime, probably
431 contributing to the relative increase in 2.5–15 nm diameter particles seen most notably between
432 midnight and 6am (Figure S2). Salimi et al. (2017) reported nocturnal new particle formation
433 events in Brisbane, Australia, finding that air masses associated with nocturnal events were
434 typically transported over the ocean before reaching their sampling site, but the relevance to our
435 study is unclear, although the maritime air might sometimes be expected to show lower temperature
436 and higher humidity than that from the land.

437

438 Support for our observations also comes from the very detailed measurement and modelling study
439 of Choi and Paulson (2016). Measuring particle number size distribution downwind of a major



440 highway, they found a positive anomaly in particle number within the first 60 m of the plume peak,
441 as the peak for the small particles appeared further downwind than the peak in accumulation mode
442 particles. They attributed this to growth of unmeasured sub-5.6 nm particles into the smallest
443 measurable size range and suggested condensational growth or self-coagulation as the mechanism
444 (Choi and Paulson, 2016). Kerminen et al. (2007) measuring near a major road in Helsinki reported
445 particle growth by condensation to be a dominant process during the road-to-ambient evolution
446 stage at nighttime in winter. They inferred that under such conditions (low wind speeds with a
447 temperature inversion), traffic-generated particle numbers were enhanced and could affect
448 submicron particle number concentrations over large areas around major roads. The distance scales
449 for such processes in both studies (Choi and Paulson, 2016; Kerminen et al., 2007) were within 100
450 m of source under the conditions of measurement but might conceivably extend over greater
451 distance scales. Similar processes of particle evolution within an aircraft exhaust plume have been
452 reported by Timko et al. (2013).

453

454 Pushpawela et al. (2018) report a phenomenon of hygroscopic particle growth at nighttime, which
455 can potentially be mistaken for new particle formation. This phenomenon was observed between
456 0.5-5.0 hours after sunset, peaking at 3.5 hours (Pushpawela et al., 2018). This would not appear to
457 explain our observations, where the peak in N/SMPS and N/BC plots (Figures S2 and S5) is
458 greatest at 3-4 am local time, which in London in winter is some 10-11 hours after sunset.
459 Additionally, such a phenomenon would be expected to be unrelated to local traffic emissions, and
460 hence more uniform across the various sites.

461

462 3.5 Spatial Distribution of Particles – Horizontal and Vertical

463 Figure 2 shows the time series of particle concentrations from the SMPS instruments throughout the
464 campaign. Clearly, as expected, the Marylebone Road site shows the highest concentrations through
465 the campaign period due to its proximity to the road traffic source. The other sites tend to track one



466 another quite closely with no consistent ranking of concentrations. There are periods such as
467 February 1st to 3rd when Regent's University well exceeds North Kensington, but at other times,
468 they are very similar (e.g. 10 – 12 February), or periods when North Kensington exceeds Regent's
469 University (e.g. 7 February) but these are few. In the former period (1 – 3 February), winds were
470 southerly and concentrations at Regent's University would be enhanced by passage of air across
471 Central London, including Marylebone Road. In the situation where concentrations were similar (10
472 – 12 February), winds were in the northerly sector, giving relatively low concentrations at all sites,
473 and rather little spatial variation. The temporal pattern at all sites showed substantial similarity
474 overall (Figure 2), including diurnal patterns (Figure 3), although the magnitude of concentrations
475 varied.

476

477 A time series of CPC particle number concentrations (Figure 8) showed that under most conditions ,
478 the number count was lowest at the BT Tower site, and that the number count at Westminster
479 University frequently exceeded that at Marylebone Road, with Regent's University lower, but
480 above the concentration at the BT Tower (Figure 8). During the period of northerly winds (8 – 12
481 February), all sites showed low concentrations with Regent's University and BT Tower similar for
482 much of the time, as for the SMPS data (Figure 2). The highest CPC count concentrations during
483 the latter were measured at Westminster University (Figure 9) which was downwind of Marylebone
484 Road at those times. The similarity seen between Westminster University and Marylebone Road
485 for much of the campaign, with concentrations far in excess of those at BT Tower is strongly
486 suggestive of continuing particle growth into the size range 2.5–14.9 nm at Westminster University
487 with re-evaporation occurring before reaching the elevated BT Tower site, as previously observed
488 by Dall'Osto et al. (2011). Elevations in N/BC data were seen at the BT Tower site (Figure S4 and
489 S5) but these occurred mainly during the morning rush hour period, presumably due to fresh traffic
490 emissions, rather than overnight as at the other sites (Figure S5).

491



492 Figure 2 suggests that vertical gradients between the proximate Regent's University and BT Tower
493 sites were small in SMPS count (Figure 2), but at certain times were substantial in the CPC count
494 (Figure 9). The particle size distributions measured at the BT Tower (Figure 4d) differ from
495 Marylebone Road and North Kensington (Figure 4a and b) in having no obvious mode in the
496 nucleation size range at 20 – 30 nm, a feature shared with Regent's University (Figure 4c). Only
497 during westerly winds (270°) does the BT Tower show such a mode (Figure 4d), while at Regent's
498 University (Figure 5) the 270° wind direction also shows differences from the others with a mode at
499 below 20 nm. Anomalous behaviour in this wind sector is also observed at North Kensington
500 (Figure 4b), and at Marylebone Road. The most pronounced nucleation mode peak is associated
501 with the 270° and 225° wind directions. In the Marylebone Road case, these wind directions are
502 almost parallel to the highway, which might explain the high concentrations and pronounced
503 nucleation mode, but this explanation does not work for the other sites. A more likely explanation is
504 that all sites are affected by emissions from Heathrow Airport which is to the west of London and
505 has been recognised as a major source of nucleation mode particles associated with aircraft and road
506 traffic emissions (Masiol et al., 2017). At a site 1 km from the northern boundary of Heathrow
507 Airport, PMF factors attributed to aircraft (mode at <20 nm) and fresh road traffic emissions (mode
508 at 18–35 nm) accounted respectively for 31.6% and 27.9% of particle number count in the warm
509 season and 33.1% and 35.2% in the cold season (December 2014 – January 2015) data (Masiol et
510 al., 2017). Heathrow Airport is located approximately 22 km from our Central London sites on a
511 bearing of 255° . Keuken et al. (2015) measured a large elevation in concentrations of particles of
512 10–20 nm diameter attributed to aircraft emissions (emission studies are reviewed by Masiol and
513 Harrison, 2014) at a site 7 km east of Schiphol Airport (Netherlands) and have shown by modelling
514 and measurement that concentrations are elevated to considerably greater downwind distances.
515 Similarly, Hudda et al. (2014) reported PNC to have increased 4 to 5 fold at 8 – 10 km downwind
516 of Los Angeles International Airport (USA).
517



518 The size distributions have also been analysed according with mixed layer height (MLH),
519 determined by ceilometer (Kotthaus and Grimmond, 2018). Both Marylebone Road (Figure S6) and
520 Regent's University (Figure S7) have the highest concentrations associated with the deepest MLH
521 class (>1000 m). This seems likely to be due to an association with southerly winds and the street
522 canyon circulation. Whereas, North Kensington (Figure S8) has the highest concentrations during
523 shallow MLH (< 100 m and 100 – 200 m) when dispersion is limited for the low altitude emissions.
524 The most interesting behaviour is seen at the elevated (160 m) BT Tower site, which is consistent
525 with Harrison et al. (2012a) and Dall'Osto et al. (2011). During the shallowest MLH (< 100 m) the
526 measurement site is above the inversion and the size distribution lacks an obvious nucleation mode
527 (Figure S9). As the MLH deepens, a nucleation mode appears which dominates the size
528 distribution for the deepest MLH categories (900 – 1000 m and >1000 m) with a mode at 20 – 30
529 nm, similar to that seen at Marylebone Road for the same MLH depths (Figure S6). The gradual
530 transition of size distribution as the MLH deepens is consistent with the surface source (mainly
531 road traffic) of nucleation mode particles, and their evaporative loss which increases with the
532 timescale of vertical mixing to the height of the sampler, as reported by Dall'Osto et al. (2011), and
533 the ultimate isolation of the sampler from ground-level emissions at the shallowest boundary layer
534 heights, as observed by Harrison et al. (2012a).

535

536 **3.6 Detailed Comparison of Marylebone Road, Westminster University and Regent's** 537 **University**

538 Unfortunately, a full dataset for the Westminster University site was only collected over the period
539 January 30th to February 1st due to a late set-up of the instrument and a malfunction after February
540 1st. This period however merits closer examination as it is the only period where SMPS data were
541 available for all three sites. For much of the time the SMPS data for the Westminster University
542 site looks surprisingly similar to that of the Marylebone Road site despite the former being on the
543 rooftop and the latter being within the street canyon. A detailed analysis hour by hour showed that



544 out of 51 hourly observations, in 23 the amplitude of the mode (dN/dlogD) at Westminster
545 University was within $\pm 20\%$ of that at Marylebone Road while in 25 cases the amplitude was
546 greater at Westminster University than at Marylebone Road, and in just two cases the amplitude
547 was smaller at Westminster University. In an attempt to explain this observation, the
548 meteorological data for the periods of similar magnitude and of different magnitudes were
549 compared but no systematic difference was seen in wind direction, air temperature or relative
550 humidity between any of the periods. Wind directions were generally in a south-easterly to easterly
551 sector, mean temperatures around 8°C and relative humidity high (85 and 99%). The maximum
552 MLH were low and there was a lot of rain (Figure S10).

553

554 In order to gain further insight, the time series of observations were plotted for this period and
555 appear in Figure 9. The SMPS integrated number counts shown in Figure 9(a) show a remarkable
556 similarity between Marylebone Road, Westminster University and Regent's University. For the
557 first two days, Regent's University concentrations are lower than those from the other two sites,
558 although on the third day they are very similar to those at Westminster University. On the first and
559 last days, the peak concentrations at Marylebone Road exceed those at Westminster University but
560 on the middle day (January 31st) the differences between these two sites are very small. The CPC
561 particle number counts shown in Figure 9(b) are very similar to those at Marylebone Road on the
562 first and last day but exceed those at Marylebone Road on January 31st. Concentrations at Regent's
563 University are typically only around half or less of those measured at Westminster University. The
564 magnitude of the CPC concentrations peaking at over $40,000\text{ cm}^{-3}$ is close to double the integrated
565 SMPS counts which peak at a little over $20,000\text{ cm}^{-3}$ indicating a large number of particles in the
566 size range below 14.9 nm.

567

568 However, the Black Carbon data (Figure 9c) have daytime concentrations at Marylebone Road that
569 far exceed those at Westminster University and Regent's University, the latter sites tracking each



570 other and having very similar concentrations. Since Black Carbon can be viewed as a conserved
571 tracer of vehicle emissions over these small time and distance scales, the inference is that particle
572 production must be continuing as the vehicle exhaust mixes upwards from the street canyon
573 Marylebone Road site to the Westminster University rooftop site. The southerly wind directions
574 likely associated with upward flow on the Westminster University canyon wall (Fig. 6) would carry
575 vehicle exhaust past the Marylebone Road measurement station (south side of the road).

576

577 Air leaving the canyon and being entrained by the complex building roof flows could expose the
578 Westminster University sampler to air exiting the street canyon and to the general flow towards
579 Regent's University site (Fig. 6 and 1). Such behaviour is consistent with the observations of
580 particle growth in the sub-SMPS size ranges reported in the previous section extending into the
581 SMPS size range. This is similar to behaviour observed by Kerminen et al. (2007) in Helsinki who
582 observed not only possibly evaporation of some particles in the 7–30 nm range, but also on apparent
583 growth of nucleation mode particles into the 30–63 nm size range between sampling points at 9 m
584 and 65 m downwind of a highway. The results in Figure 9 are suggestive of a substantial growth of
585 nuclei into the range of the CPC at Westminster University.

586

587 **4. CONCLUSIONS**

588 The measurement of particle number size distributions in the atmosphere is resource intensive and
589 there have been rather few studies in which more than two samplers have been operated within a
590 city. Typically if there are two sites, one is a traffic-influenced site and the other urban background.
591 In this study, data have been collected at a total of five sites, although unfortunately the dataset
592 from the Westminster University site is limited to only a few days. Nonetheless, the dataset allows
593 some deep insights into the spatial distribution of particle sizes and number counts not only
594 horizontally but in the vertical dimension. Not unexpectedly, concentrations of particles at the
595 street canyon Marylebone Road site considerably exceed concentrations at other sites, but there are



596 nonetheless considerable similarities in diurnal profiles and the magnitude of concentrations at the
597 other, background sites.

598

599 One of the main motivating factors for this study was to confirm earlier observations of shrinkage
600 of the nucleation mode particles between traffic emissions on Marylebone Road and the downwind
601 site at Regent's University within Regent's Park. Particle shrinkage was observed within the
602 current study although at a slower mean rate (0.04nm s^{-1}) than in the earlier study (Harrison et al.,
603 2016) in which the mean shrinkage rate was 0.13nm s^{-1} . However, temperatures in the current
604 study all fell below those in the earlier work of Harrison et al. (2016). Other factors may also have
605 been influential. There have been marked changes in the road vehicle fleet in London between the
606 two measurement campaigns. The earlier dataset as reported by Dall'Osto et al. (2011) and
607 Harrison et al. (2016) was collected in 2006 at which time the sulphur content of diesel fuel was
608 regulated at below 50 ppm. Between the two campaigns, the sulphur content of both gasoline and
609 diesel motor fuels was reduced to below 10 ppm sulphur in order to facilitate the introduction of
610 diesel particle filters from 2011 onwards. The incorporation of a diesel particle filter on EURO 5
611 and EURO 6 vehicles leads to a substantial overall reduction in particulate matter emissions but
612 also a change in the hydrocarbon content of the particles. Secondly, the Regent's Park sampling
613 site used for the 2006 measurements was at about double the distance from Marylebone Road
614 compared to the Regent's University used in the latest study. This would allow for greater dilution
615 of the traffic plume from Marylebone Road and other adjacent highways, leading to a greater
616 reduction in vapour phase hydrocarbons at the more distant site causing an accelerated evaporation
617 process. The reduction in fuel sulphur content in 2007 was accompanied by a marked change in the
618 size distribution of particles emitted from road traffic, including a reduction in the nucleation mode
619 particles (Jones et al., 2012). The work of Dall'Osto et al. (2011) also analysed data from the BT
620 Tower, showing increasing evaporative loss of nucleation mode particles as the travel time from
621 ground level to the sampling site on the Tower became longer with reduced atmospheric turbulence



622 levels. Although that phenomenon has not been studied in detail in the latest dataset, the results are
623 clearly consistent with such a process, and with an apparent total loss of the nucleation mode in
624 particles associated with regional pollution sampled when the boundary layer top was below the
625 sampling height on the tower.

626

627 Although the phenomenon of particle shrinkage had been seen in earlier work, there were two
628 further major observations made in the current study which were not anticipated. The first, was the
629 clear influence of a major source to the west of London, almost certainly Heathrow Airport, upon
630 concentrations of nucleation mode particles. The association of an enhanced nucleation mode in the
631 270° or 225° sector is indicative of a major source of very fine particles, and the work of Masiol et
632 al. (2017) at a sampling site close to Heathrow Airport provides strong evidence for major
633 emissions both from aircraft engines and the large volumes of road traffic attracted by the airport.
634 Earlier research by Keuken et al. (2015) and Hudda et al. (2014) gives a clear precedent for
635 measurement of strongly elevated concentrations of very fine particles several kilometres
636 downwind of a major airport, but to our knowledge this is the first observations of concentrations
637 above urban background at a distance of 22 km from the centre of the airport.

638

639 The other observation which was wholly unexpected was of the very poor relationship between total
640 particle numbers measured by the Scanning Mobility Particle Sizers and the total particle numbers
641 measured by co-located condensation particle counters. While both the SMPS counts and co-
642 located Black Carbon measurements show a typical road traffic diurnal profile, the CPC data show
643 a quite different diurnal profile peaking at night. This is most evident in the ratios of CPC/SMPS
644 and CPC/BC seen at all sampling sites, with the exception of CPC/BC at the elevated BT Tower
645 site which does not show a nocturnal maximum, but peaks during the morning rush hour period.
646 Earlier studies such as that of Choi and Paulson (2016) and Kerminen et al. (2007) have reported
647 data consistent with such a phenomenon, but with very modest elevations in particle count



648 compared to those in the current data. The implication is of the presence of large numbers of
649 particles within the range of 2.5 – 15nm and hence observable with the CPC but below the lower
650 cut of the SMPS. It seems likely that such particles grow at night from vary small nuclei and it
651 seems possible that the exceptional magnitude of this process within London results from the high
652 density of diesel traffic leading to substantial nocturnal concentrations of condensable vapours close
653 to the traffic source. A common feature to such observations appears to be its association with still
654 conditions on winter nights which lead to poor dispersion of vehicle emissions and a pool of vapour
655 co-emitted with traffic particles which becomes supersaturated as it cools in the ambient
656 atmosphere, leading to condensation on small nuclei when the general particle concentrations and
657 hence the condensation sink are relatively low in magnitude.

658

659 These very abundant particles within the 2.5 – 15 nm range are likely to prove ephemeral as they
660 would be expected to re-evaporate as the air mass dilutes away from source. However, the health
661 effects of exposure to particles within this range are poorly known and no recommendation can be
662 given as to whether health-related studies would be best to measure the particle size range covered
663 by the SMPS as is most typically performed at present, or whether CPC data going down to smaller
664 particles sizes would be more appropriate.

665

666 There are some additional general conclusions from the work. Firstly the results demonstrate the
667 dynamic behaviour of traffic-generated (and other) particles within the urban atmosphere. Our
668 earlier paper (Dall'Osto et al., 2011) referred to “remarkable dynamics”, and further remarkable
669 dynamic processes have been observed in the current study. Secondly, as this work has revealed
670 sources and processes that were not originally anticipated, although with the benefit of hindsight it
671 might have been possible to predict them, there is clearly a need for further detailed observational
672 studies of the behaviour of sub-100 nm particles within the urban atmosphere.

673



674 **ACKNOWLEDGEMENTS**

675 The authors are grateful to the management and staff of Westminster University, Regent's
676 University and British Telecom for access to their buildings for air sampling. They also express
677 gratitude to the National Centre for Atmospheric Science (NCAS) for the loan of sampling
678 instruments, and to Dr Paul Williams (NCAS) for facilitating the instrument intercomparison. The
679 operation of the ceilometers were supported by NERC ClearfLo, NERC AirPro, Newton Fund/Met
680 Office CSSP (SG, SK) and University of Reading. We acknowledge the support of KCL LAQN for
681 the instrument sites and support and the Reading Urban Micromet group for maintaining the
682 instruments, notably in this period Elliott Warren and Kjell zum Berge. The work was funded by the
683 European Research Council (ERC-2012-AdG, Proposal No. 320821) and the UK Natural
684 Environment Research Council (R8/H12/83/011) and a NCAS studentship (to JB).

685

686

687

688 **REFERENCES**

689

690 Agus, E. L., Young, D. T., Lingard, J. J. N., Smalley, R. J., Tate, J. E., Goodman, P. S., and Tomlin,
691 A. S.: Factors influencing particle number concentrations, size distributions and modal parameters
692 at a roof-level and roadside site in Leicester, UK, *Sci. Tot. Environ.*, 386, 65-82, 2007.

693

694 Alam, M. S., Rezaei, S. Z., Stark, C. P., Liang, Z., Xu, H. M., and Harrison R. M.: The
695 characterisation of diesel exhaust particles – composition, size distribution and partitioning, *Faraday*
696 *Discuss.*, 189, 69-84, 2016.

697

698 Beddows, D. C. S., Dall'Osto, M., Harrison, R. M., Kulmala, M., Asmi, A., Wiedensohler, A., Laj,
699 P., Fjaeraa, A. M., Sellegri, K., Birmili, W., Bukowiecki, N., Weingartner, E., Baltensperger, U.,
700 Zdimal, V., Zikova, N., Putaud, J.-P., Marinoni, A., Tunved, P., Hansson, H.-C., Fiebig, M.,
701 Kivekäs, N., Swietlicki, E., Lihavainen, H., Asmi, E., Ulevicius, V., Aalto, P.P., Mihalopoulos, N.,
702 Kalivitis, N., Kalapov, I., Kiss, G., De Leeuw, G., Henzing, B., O'Dowd, C., Jennings, S. G.,
703 Flentje, H., Meinhardt, F., Ries, L., Denier Van Der Gon, H. A. C., and Visschedijk, A. J. H.:
704 Variations in tropospheric submicron particle size distributions across the European Continent
705 2008-2009. *Atmos. Chem. Phys.*, 14, 4327-4348, 2014.

706

707 Beddows, D. C. S., and Harrison, R. M., Green, D., Fuller, G.: Receptor modelling of both particle
708 composition and size distribution data from a background site in London UK, *Atmos. Chem. Phys.*,
709 15, 10107-10125, 2015.

710

711 Bigi, A., and Harrison R. M.: Analysis of the air pollution climate at a central urban background
712 site, *Atmos. Environ.*, 44, 2004-2012, 2010.

713

714 Bohnenstengel, S. I., Belcher, S. E., Aiken, A., Allan, J. D., Allen, G., Bacak, A., Bannan, T. J.,
715 Barlow, J. F., Beddows, D. C. S., Bloss, W. J., Booth, A. M., Chemel, C., Coceal, O., Di Marco, C.
716 F., Dubey, M. K., Faloon, K. H., Fleming, Z. L., Furger, M., Geitl, J. K., Graves, R. R., Green, D.
717 C., Grimmond, C. S. B., Halios, C. H., Hamilton, J. F., Harrison, R. M., Heal, M. R., Heard, D. E.,
718 Helfter, C., Herndon, S. C., Holmes, R. E., Hopkins, J. R., Jones, A. M., Kelly, F. J., Kotthaus, S.,
719 Langford, B., Lee, J. D., Leigh, R. J., Lewis, A. C., Lidster, R. T., Lopez-Hilfiker, F. D., McQuaid,
720 J. B., Mohr, C., Monks, P. S., Nemitz, E., Ng, N. L., Percival, C. J., Prévôt, A. S. H., Ricketts, H.
721 M. A., Sokhi, R., Stone, D., Thornton, J. A., Tremper, A. H., Valach, A. C., Visser, S., Whalley, L.
722 K., Williams, L. R., Xu, L., Young, D. E., and Zotter, P.: Meteorology, air quality, and health in
723 London: The ClearfLo project. *Amer. Meteor. Soc.*, 779-804, 2015.

724

725 Carslaw, D. C., and Ropkins, K.: openair – An R package for air quality data analysis, *Environ.*
726 *Model. Softw.* 27-28, 52-61, doi:<https://doi.org/10.1016/j.envsoft.2011.09.008>, 2012.

727

728 Charron, A., and Harrison, R. M.: Primary particle formation from vehicle emissions during
729 exhaust dilution in the roadside atmosphere, *Atmos. Environ.*, 37, 4109-4119, 2003.

730

731 Choi W., and Paulson, S. E.: Closing ultrafine particle number concentration budget at road-to-
732 ambient scale: Implications for particle dynamics, *Aerosol Sci. Technol.*, 50, 5, 448-461, 2016.

733

734 Crilley, L. R., Bloss, W. J., Yin, J., Beddows, D. C. S., Harrison, R. M., Allan, J. D., Young, D. E.,
735 Flynn, M., Williams, P., Zotter, P., Prevot, A. S. H., Heal, M. R., Barlow, J. F., Hallios, C. H., Lee,
736 J. D., Szidat, S., and Mohr, C.: Sources and contributions of wood smoke during winter in London:
737 assessing local and regional influences, *Atmos. Chem. Phys.*, 15, 3149-3171, 2015.

738



- 739 Dall'Osto, M., Thorpe, A., Beddows, D.C.S., Harrison, R.M., Barlow, J.F., Dunbar, T., Williams,
740 P.I., and Coe, H.: Remarkable dynamics of nanoparticles in the urban atmosphere, *Atmos. Chem.*
741 *Phys.*, 11, 6623-6637, 2011.
- 742
- 743 Enroth, J., Saarikoski, S., Niemi, J., Kouse, A., Jezek, I., Mocnik, G., Carbone, S., Kuulivainen, H.,
744 Rönkkö, T., Hillamo, R., and Pirjola, L.: Chemical and physical characterization of traffic particles
745 in four different highway environments in the Helsinki metropolitan area, *Atmos. Chem. Phys.*, 16,
746 5497-5512, 2016.
- 747
- 748 Harrison, R.M., Shi, J.P., Xi, S., Khan, A., Mark, D., Kinnersley, R., and Yin, J.: Measurement of
749 number, mass and size distribution of particles in the atmosphere, *Phil. Trans. R. Soc. Lond.*, A,
750 358, 2567-2580, 2000.
- 751
- 752 Harrison, R.M., Beddows, D.C., and Dall'Osto, M.: PMF analysis of wide-range particle size
753 spectra collected on a major highway, *Environ. Sci. Technol.*, 45, 5522-5528, 2011.
- 754
- 755 Harrison, R.M., Dall'Osto, M., Beddows, D.C.S., Thorpe, A.J., Bloss, W.J., Allan, J.D., Coe, H.,
756 Dorsey, J.R., Gallagher, M., Martin, C., Whitehead, J., Williams, P.I., Jones, R.L., Langridge, J.M.,
757 Benton, A.K., Ball, S.M., Langford, B., Hewitt, C.N., Davison, B., Martin, D., Petersson, K.,
758 Henshaw, S.J., White, I.R., Shallcross, D.E., Barlow, J.F., Dunbar, T., Davies, F., Nemitz, E.,
759 Phillips, G.J., Helfter, C., Di Marco, C.F., and Smith, S.: Atmospheric chemistry and physics in the
760 atmosphere of a developed megacity (London): An overview of the REPARTEE experiment and its
761 conclusions, *Atmos. Phys. Chem.*, 12, 3065-3114, 2012a.
- 762
- 763 Harrison, R.M., Beddows, D.C.S., Hu, L., and Yin, J.: Comparison of methods for evaluation of
764 wood smoke and estimation of UK ambient concentrations, *Atmos. Chem. Phys.*, 12, 8271-8283,
765 2012b.
- 766
- 767 Harrison, R.M., Jones, A.M., Beddows, D.C., and Dall'Osto, M.: Evaporation of traffic-generated
768 nanoparticles during advection from source, *Atmos. Environ.*, 125, 1-7, 2016.
- 769
- 770 HEI: Understanding the Health Effects of Ambient Ultrafine Particles, Health Effects Institute, HEI
771 Perspectives 3, 2013.
- 772
- 773 Herner, D.H., Hu, S., Robertson, W.H., Huai, T., Chang, M.C.O., Riger, P., and Ayala, A.: Effect
774 of Advanced Aftertreatment for PM and NO_x Reduction on Heavy-Duty Diesel Engine Ultrafine
775 Particle Emissions, *Environ. Sci. Technol.*, 45, 2413-2419, 2011.
- 776
- 777 Hudda, N., Gould, T., Hartin, K., Larson, T.V., and Fruin, S.A.: Emissions from an international
778 airport increase particle number concentrations 4-fold at 10km downwind, *Environ. Sci. Technol.*,
779 48, 6628-6635, 2014.
- 780
- 781 Hussein, T., Karppinen, A., Kukkonen, J., Harkonen, J., Aalto, P.P., Hameri, K., Kerminen, V.-M.,
782 and Kulmala, M.: Meteorological dependence of size-fractionated number concentrations of urban
783 aerosol particles, *Atmos. Environ.*, 40, 1427-1440, 2006.
- 784
- 785 Jones, A.M., Harrison, R.M., Barratt, B., and Fuller, G.: A large reduction in airborne particle
786 number concentrations at the time of the introduction of "sulphur free" diesel and the London Low
787 Emission Zone, *Atmos. Environ.*, 50, 129-138, 2012.
- 788
- 789 Kerminen, V.M., Pakkanen, T.A., Makela, T., Hillamo, R.E., Sillanpaa, M., Rönkkö, T., Virtanen,
790 A., Keskinen, J., Pirjola, L., Hussein, T., and Hameri, K.: Development of particle number size



- 791 distribution near a major road in Helsinki during an episodic inversion situation, *Atmos. Environ.*,
792 41, 1759-1767, 2007.
- 793
- 794 Ketzel, M., Wahlin, P., Berkowicz, R., and Palmgren, F.: Particle and trace gas emission factors
795 under urban driving conditions in Copenhagen based on street and roof-level observations, *Atmos.*
796 *Environ.*, 37, 2735-2749, 2003.
- 797
- 798 Keuken, M.P., Moerman, M., Zandveld, P., Henzing, J.S., and Hoek, G.: Total and size-resolved
799 particle number and Black Carbon concentrations in urban areas near Schiphol airport (the
800 Netherlands), *Atmos. Environ.*, 104, 132-142, 2015.
- 801
- 802 Kontkanen, J., Lehtipalo, K., Ahonen, L., Kangaslua, J., Manninen, H.E., Hakala, J., Rose, C.,
803 Sellegri, K., Xiao, S., Wang, L., Qi, X., Nie, W., Ding, A., Yu, H., Lee, S., Kerminen, V.-M.,
804 Petaja, T., and Kulmal, M.: Measurements of sub-3 nm particles using a particle size magnifier in
805 different environments: from clean mountain top to polluted megacities, *Atmos. Chem. Phys.*, 17,
806 2163-2187, 2017.
- 807
- 808 Kotthaus S, and Grimmond, C.S.B.: Atmospheric boundary layer characteristics from ceilometer
809 measurements Part 1: A new method to track mixed layer height and classify clouds, *Q. J. R.*
810 *Meteorol. Soc.*, <https://doi.org/10.1002/qj.3299>, 2018.
- 811
- 812 Kotthaus, S., and Grimmond, C. S. B.: Atmospheric boundary layer characteristics from ceilometer
813 measurements, Part 2: Application to London's urban boundary layer, *Q. J. R. Meteorol. Soc.*,
814 <https://doi.org/10.1002/qj.3298>, 2018.
- 815
- 816 Kotthaus, S., Halios, C. H., Barlow, J. F., and Grimmond, C.S.B.: Volume for pollution dispersion:
817 London's atmospheric boundary layer during ClearfLo observed with two ground-based lidar types
818 *Atmos. Environ.*, 190, 401-414, 2018.
- 819
- 820 Kumar, P., Fennell, P., and Britter, R.: Measurements of particles in the 5-1000 nm range close to
821 road level in an urban street canyon, *Sci. Tot. Environ.*, 390, 437-447, 2008a.
- 822
- 823 Kumar, P., Fennell, P., Langley, D., and Britter, R.: Pseudo-simultaneous measurements for the
824 vertical variation of coarse, fine and ultrafine particles in an urban street canyon, *Atmos. Environ.*,
825 42, 4304-4319, 2008b.
- 826
- 827 Kumar, P., Garmory, A., Ketzel, M., Berkowicz, R., and Britter, R.: Comparative study of
828 measured and modelled number concentrations of nanoparticles in an urban street canyon, *Atmos.*
829 *Environ.*, 43, 949-958, 2009.
- 830
- 831 Li, X. L., Wang, J. S., Tu, X. D., Liu, W., and Huang, Z.: Vertical variations of particle number
832 concentration and size distribution in a street canyon in Shanghai, China, *Sci. Tot. Environ.*, 378,
833 306-316, 2007.
- 834
- 835 Lingard, J. J. N., Agus, E.L., Young, D. T., Andrew, G. E., and Tomlin, A. S.: Observations of
836 urban airborne particle number concentrations during rush-hour conditions: analysis of the number
837 based size distributions and modal parameters, *J. Environ., Monitor.*, 8, 1203-1218, 2006.
- 838
- 839 Longley, I. D., Gallagher, M. W., Dorsey, J. R., Flynn, M., Allan, J. D., Alfarra, M. R., and Inglis,
840 D.: A case study of aerosol ($4.6 \text{ nm} < D_p < 10 \text{ }\mu\text{m}$) number and mass size distribution measurements
841 in a busy street canyon in Manchester, UK, *Atmos. Environ.*, 37, 1563-1571, 2003.
- 842



- 843 Masiol, M., and Harrison, R. M.: Aircraft engine exhaust emissions and other airport-related
844 contributions to ambient air pollution: A review, *Atmos. Environ.*, 95, 409-455, 2014.
845
- 846 Masiol, M., Harrison, R. M., Tuan, V. V., and Beddows, D. C. S.: Sources of sub-micrometre
847 particles near a major international airport, *Atmos. Chem. Phys.*, 17, 12379-12403, 2017.
848
- 849 Nikolova, I., Janssen, S., Vos, P., Vrancken, K., Mishra, V., and Berghmans, P.: Dispersion
850 modelling of traffic induced ultrafine particles in a street canyon in Antwerp, Belgium and
851 comparison with observations, *Sci. Tot. Environ.*, 412, 336-343, 2011.
852
- 853 Nosko, O., Vanhanen, J., and Olofsson, U.: Emission of 1.3-10 nm airborne particles from brake
854 materials, *Aerosol Sci. Technol.*, 51, 91-96, 2017.
855
- 856 NPL: Design, construction and testing of a humidity management system for ultrafine particle field
857 measurements, National Physical Laboratory, NPL Report AS 48, 2010.
858
- 859 Oke, T., Mills, G., Christen, A., and Voogt, J.: *Urban Climates*, Cambridge University Press,
860 doi:10.1017/9781139016476, 2017.
861
- 862 Olivares, G., Johansson, C., Strom, J., and Hansson, H.-C.: The role of ambient temperature for
863 particle number concentrations in a street canyon, *Atmos. Environ.*, 41, 2145-2155, 2007.
864
- 865 Pushpawela, B., Jayaratne, R., and Morawska, L.: Differentiating between particle formation and
866 growth events in an urban environment, *Atmos. Chem. Phys.*, 18, 11171-11183, 2018.
867
- 868 Rönkkö, T., Virtanen, A., Vaaraslahti, K., Keskinen, J., Pirjola, L., and Lappi, M.: Effect of
869 dilution conditions and driving parameters on nucleation mode particles in diesel exhaust:
870 Laboratory and on-road study, *Atmos. Environ.*, 40, 2893-2901, 2006.
871
- 872 Rönkkö, T., Kuuluvainen, H., Karjalainen, P., Keskinen, J., Hillamo, R., Niemi, J. V., Pirjola,
873 L., Timonen, H. J., Saarikoski, S., Saukko, E., Järvinen, A., Silvennoinen, H., Rostedt, A., Olin,
874 M., Yli-Ojanperä, J., Nousiainen, P., Koussa, A., and Dal Maso, M.: Traffic is a major source of
875 atmospheric nanocluster aerosol, *PNAS*, 114, 7549-7554, 2017.
876
- 877 Salimi, F., Rahman, Md. M., Clifford, S., Ristovski, Z., and Morawska, L.: Nocturnal new particle
878 formation events in urban environments, *Atmos. Chem. Phys.*, 17, 521-530, 2017.
879
- 880 Schneider, J., Hock, N., Weimer, S., Borrmann, S., Kirchner, U., Vogt, R., and Scheer, V.:
881 Nucleation Particles in Diesel Exhaust: Composition Inferred from In Situ Mass Spectrometric
882 Analysis, *Environ. Sci. Technol.*, 39, 6153-6161, 2005.
883
- 884 Shi, J. P., and Harrison, R. M.: Investigation of ultrafine particle formation during diesel exhaust
885 dilution, *Environ. Sci. Technol.*, 33, 3730-3736, 1999.
886
- 887 Shi, J. P., Mark, D., and Harrison, R. M.: Characterization of Particles from a Current Technology
888 Heavy-Duty Diesel Engine, *Environ. Sci. Technol.*, 34, 748-755, 2000.
889
- 890 Shi, J. P., Evans, D. E., Khan, A. A., and Harrison, R. M.: Sources and concentration of
891 nanoparticles (< 10 nm diameter) in the urban atmosphere, *Atmos. Environ.*, 35, 1193-1202, 2001.
892



- 893 Timko, M. T., Fortner, E., Franklin J., Yu, Z., Wong, W., Onasch, T. B., Miake-Lye, R. C., and
894 Herndon, S. C.: Atmospheric Measurements of the Physical Evolution of Aircraft Exhaust Plumes,
895 Environ. Sci. Technol, 2013, 47, 3513-3520, 2013.
896
- 897 Vakeva, M., Hameri, K., Kulmala, M., Lahdes, R., Ruuskanen, J., Laitinen, T.: Street level versus
898 rooftop concentrations of submicron aerosol particles and gaseous pollutants in an urban street
899 canyon, Atmos. Environ., 33, 1385-1397, 1999.
900
- 901 Villa, T. F., Jayaratne, E. R., Gonzalez, L. F., and Morawska, L.: Determination of the vertical
902 profile of particle number concentration adjacent to a motorway using an unmanned aerial vehicle,
903 Environ. Pollut., 230, 143-142, 2017.
904
- 905 Vu, T. V., Delgado-Saborit, J. M., and Harrison, R. M.: Review: Particle number size distributions
906 from seven major sources and implications for source apportionment studies, Atmos. Environ., 122,
907 114-132, 2015a.
908
- 909 Vu, T. V., Delgado-Saborit, J. M., Harrison, R. M.: A review of hygroscopic growth factors of
910 submicron aerosols from different sources and its implication for calculation of lung deposition
911 efficiency of ambient aerosol, Air Qual. Atmos. Health, doi 10.1007/s11869-015-0365-0, 2015b.
912
- 913 Wehner, B., Birmili, W., Gnauk, T., and Wiedensohler, A.: Particle number size distributions in a
914 street canyon and their transformation into the urban-air background: measurements and a simple
915 model study, Atmos. Environ., 36, 2215-2223, 2002.
916
- 917 WHO: Air Quality Guidelines – Global Update 2005, World Health Organization, Copenhagen,
918 2006.
919
- 920 WHO: Review of Evidence on Health Aspects of Air Pollution – REVIHAAP Project, World
921 Health Organization, Copenhagen, 2013.
922
- 923 Wiedensohler, A., Birmili, W., Nowak, A., Sonntag, A., Weinhold, K., Merkel, M., Wehner, B.,
924 Tuch, T., Pfeifer, S., Fiebig, M., Fjaraa, A.M., Asmi, E., Sellegri, K., Depuy, R., Venzac, H.,
925 Villani, P., Laj, P., Aalto, P., Ogren, J.A., Swietlicki, E., Williams, P., Roldin, P., Quincey, P.,
926 Hüglin, C., Fierz-Schmidhauser, R., Gysel, M., Weingartner, E., Riccobono, F., Santos, S.,
927 Gruning, C., Faloon, K., Beddows, D., Harrison, R.M., Monahan, C., Jennings, S.G., O’Dowd, C.
928 D., Marinoni, A., Horn, H.-G., Keck, L., Jiang, J., Scheckman, J., McMurry, P. H., Deng, Z., Zhao,
929 C. S., Moerman, M., Henzing, B., de Leeuw, G., Loschau, G., and Bastian, S.: Mobility particle
930 size spectrometers: harmonization of technical standards and data structure to facilitate high quality
931 long-term observations of atmospheric particle number size distributions, Atmos. Meas. Tech., 5,
932 657-685, 2012.
933
- 934 Wojdyr M.: Fityk: A General purpose peak fitting program, J. Appl. Cryst., 43, 1126-1128, 2010.
935
- 936 Zhu, Y., Hinds, W. C., Kim, S., Shen, S., and Sioutas, C.: Study of ultrafine particles near a major
937 highway with heavy-duty diesel traffic, Atmos. Environ., 36, 4323-4335, 2002.
938



939 **TABLE LEGENDS**

940

941 **Table 1:** Location sites of instruments during the campaign. Mean sea level (msl), Above
942 ground level (agl), Condensation particle counter (CPC), Scanning Mobility Particle
943 Sizers (SMPS).

944

945

946 **FIGURE LEGENDS**

947

948 **Figure 1:** Study area locations (a) in central London (UK) and (b) more detail of the Marylebone
949 Road (MR), Westminster University (WU) and Regent's University (RU) sites.

950

951 **Figure 2:** Time series of total particle number count from the SMPS instruments at the five sites
952 (Fig. 1, Table 1) over the campaign period.

953

954 **Figure 3:** Campaign-average diurnal variation of particle number counts derived from the SMPS
955 instruments with median (line) and inter-quartile range (shading) shown.

956

957 **Figure 4:** Average particle number size distributions stratified by 45° wind directions sectors (°,
958 measured at LHR, value indicates mid-point of sector) for (a) Marylebone Road,
959 (b) North Kensington (c) Regent's University, (d) BT Tower.

960

961 **Figure 5:** Lognormal modes fitted to the average particle size spectrum at North Kensington
962 for wind direction sector 270°.

963 **Figure 6:** A schematic diagram of the wind flows in the street canyon of Marylebone Road (6
964 traffic lanes) during southerly and northerly winds. The orange marker represents the
965 MR sampling site and red marker represents the WM sampling site.

966

967 **Figure 7:** Time series (15 min) of ratio of total particle number counts, CPC/SMPS, for four
968 sites over the campaign period.

969

970 **Figure 8:** Time series (15 min) of total particle number count from the CPC instruments located
971 at four sites over the campaign period.

972

973 **Figure 9:** Time series (15 min) of (a) SMPS integrated counts, (b) particle number counts (CPC)
974 and (c) Black Carbon from Marylebone Road, Westminster University and Regent's
975 University for 30 January to 1 February 2017.

976

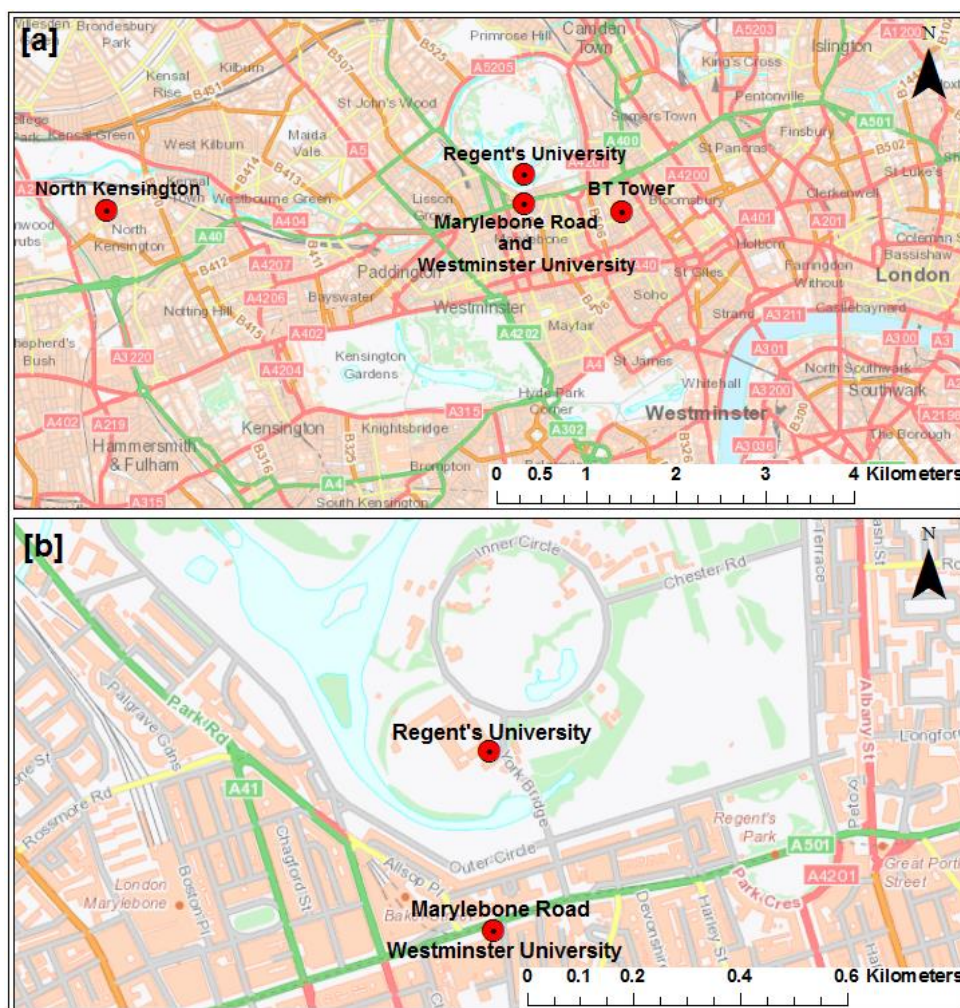
977

978



Table 1: Location sites of instruments during the campaign. Mean sea level (msl), Above ground level (agl), Condensation particle counter (CPC), Scanning Mobility Particle Sizers (SMPS).

Site Name	Marylebone Road	Westminster University	Regent's University	BT Tower	North Kensington
Lat (° N), Long (°W)	51.522530, 0.154611	51.522322, 0.15515	51.525542, 0.154570	51.521426, 0.138924	51.521082, 0.213403
Height of ground msl (m)	26	26	30	25	23
Height of inlets agl (m)	4	26	17	160	3
Instruments installed	Long_DMA_SMPS/CPC Vaisala CL31	Long_DMA_SMPS/CPC/ (Micro)Aethalometer/Anemometer	Long_DMA_SMPS/ Short_DMA_SMPS/ CPC/Aethalometer/Anemometer	Long_DMA_SMPS/CPC/ (Micro) Aethalometer/Anemometer	Long_DMA_SMPS Vaisala CL31
Particle spectrometer type	3080+3081+3775	3080+3081+3776	(3082+3081+3775)/(3082+3085+3776)	(3080+3081+3775)	(3080+3081+3775)
Aerosol dryer	Yes	No	No	No	Yes
CPC type	TSI 3025	TSI 3776	TSI 3776	TSI 3775	None



983

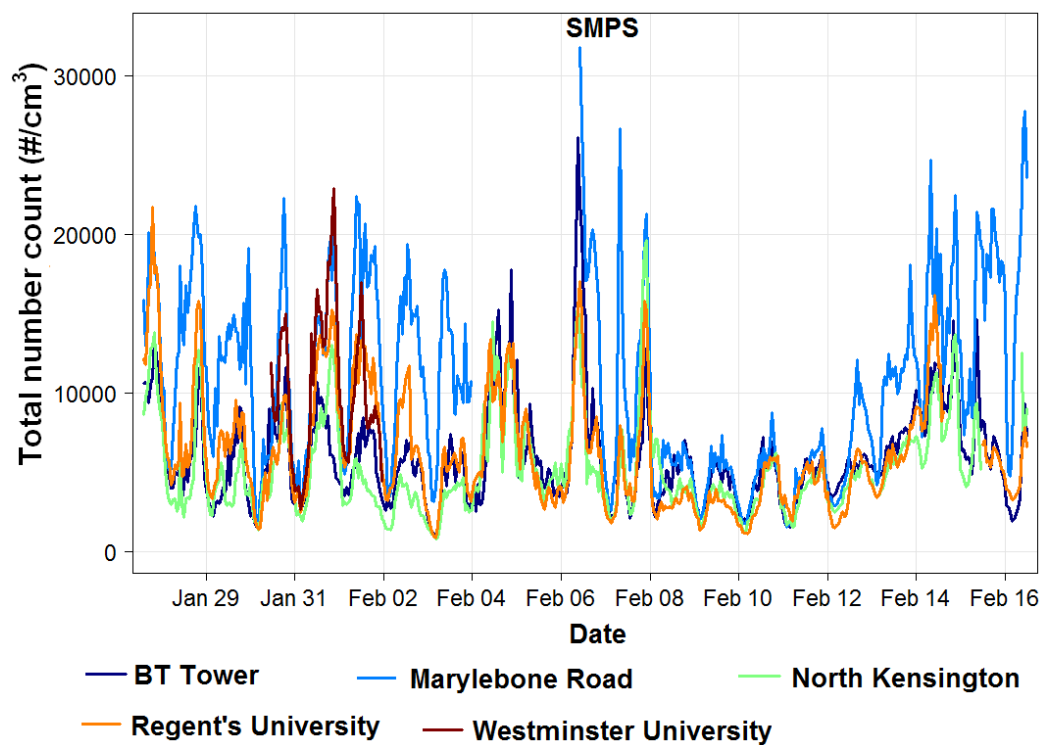
984 **Figure 1:** Study area locations (a) in central London (UK) and (b) more detail of the Marylebone
985 Road (MR), Westminster University (WU) and Regent's University (RU) sites.

986

987



988



989

990

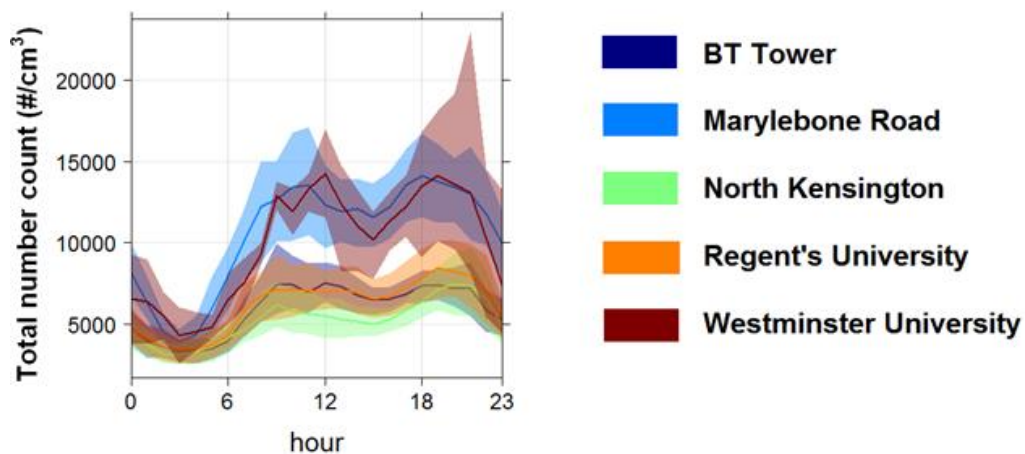
991 **Figure 2:** Time series of total particle number count from the SMPS instruments at the five sites
992 (Fig. 1, Table 1) over the campaign period.

993

994



995
996
997

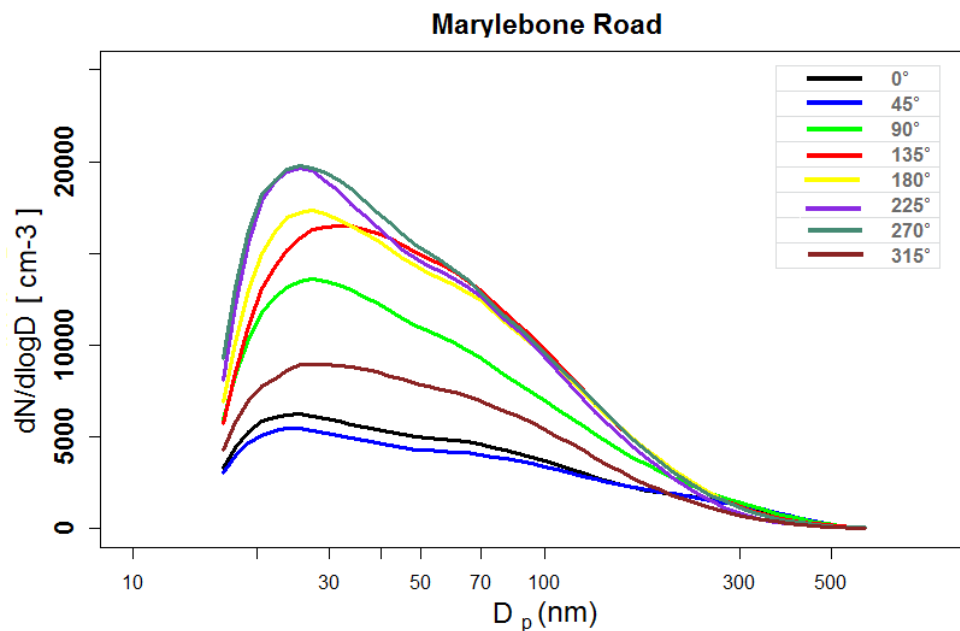


998
999
1000
1001
1002
1003
1004
1005
1006
1007

Figure 3: Campaign-average diurnal variation of particle number counts derived from the SMPS instruments with median (line) and inter-quartile range (shading) shown.

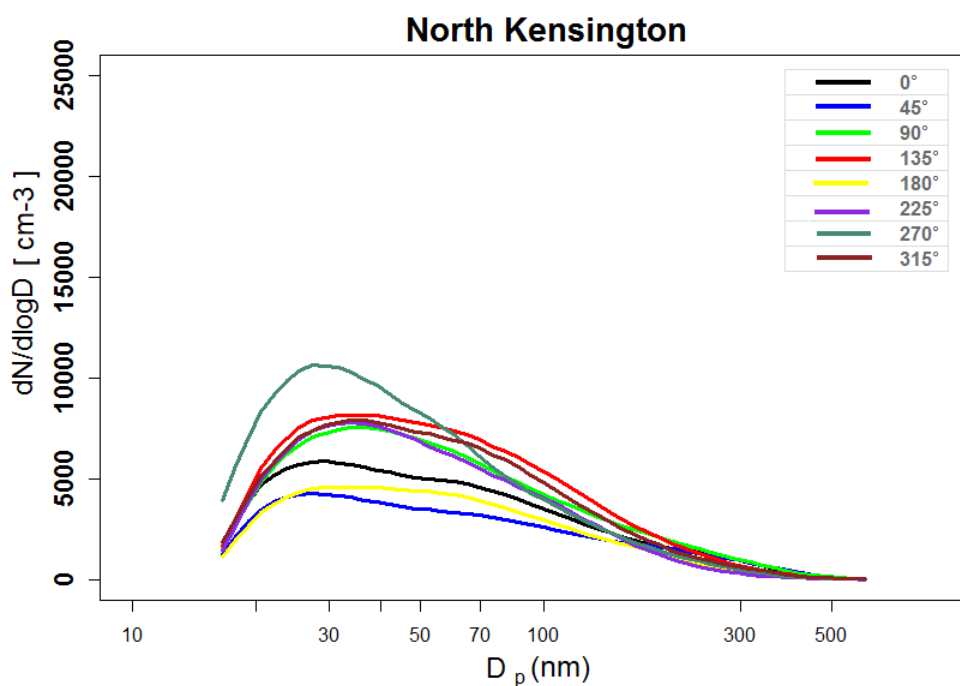


(a)



1008

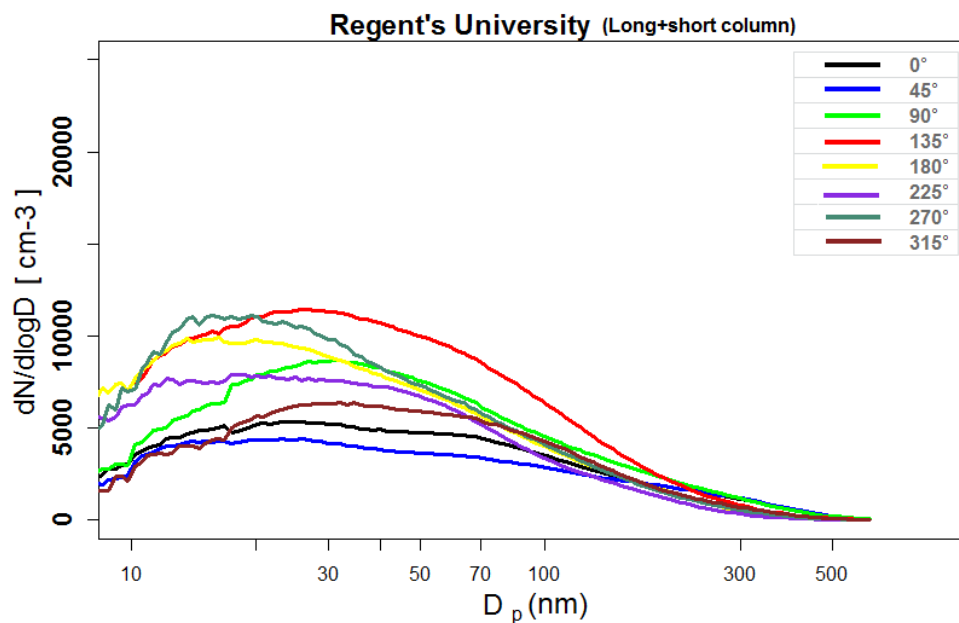
(b)



1010
1011

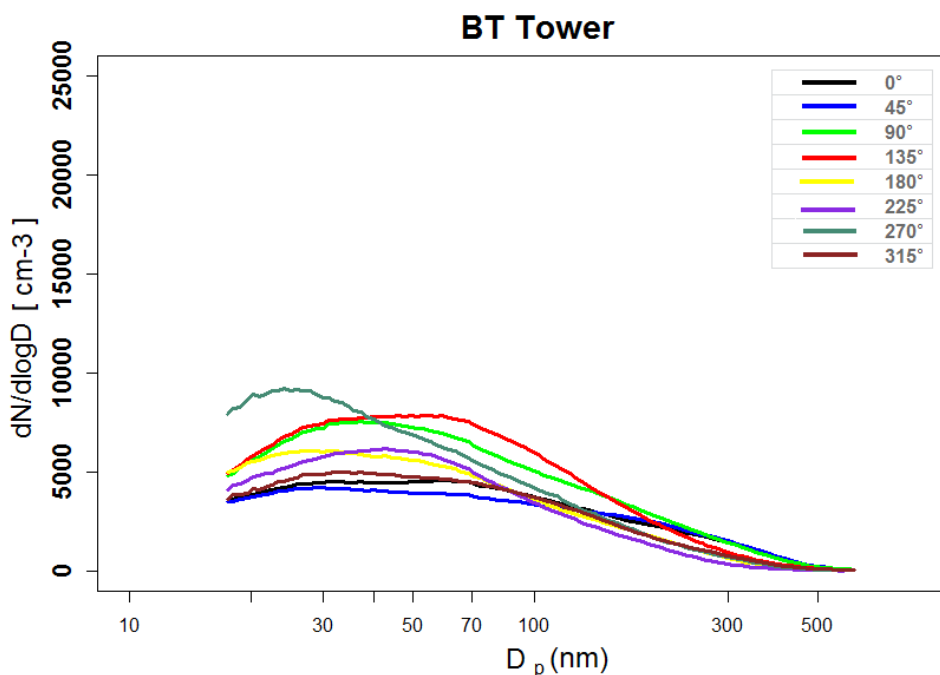


1012



1013
1014

(a)

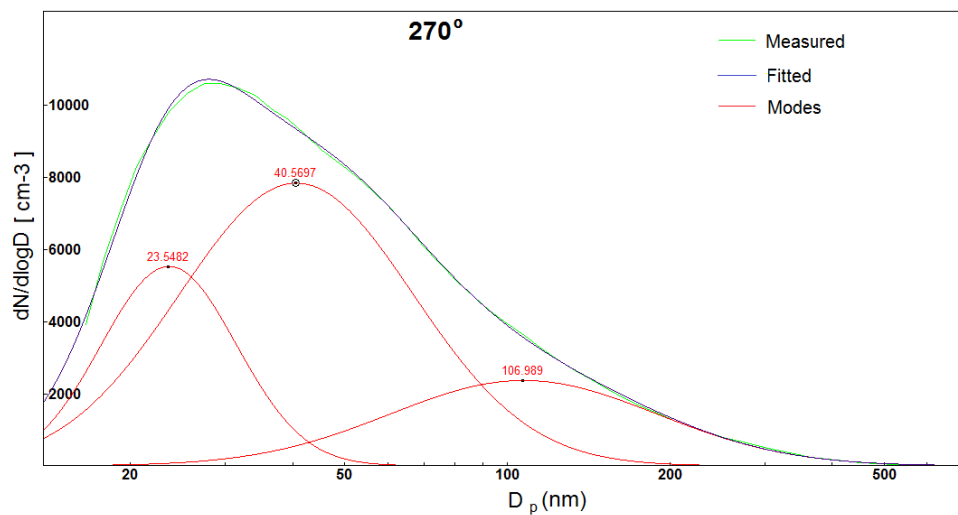


1015
1016

1017 **Figure 4:** Average particle number size distributions stratified by 45° wind directions sectors (°,
1018 measured at LHR, value indicates mid-point of sectors) for (a) Marylebone Road, (b) North
1019 Kensington (c) Regent's University, (d) BT Tower.



1020



1021

1022

1023

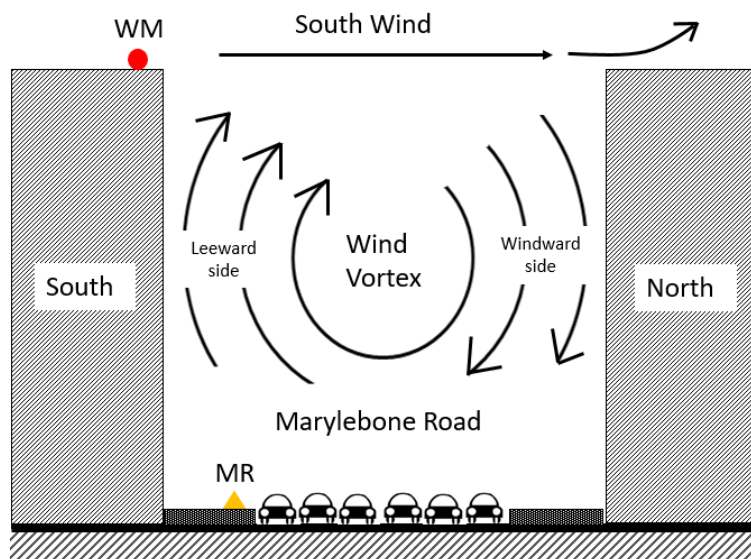
Figure 5: Lognormal modes fitted to the average particle size spectrum at North Kensington for wind direction sector 270°.

1024

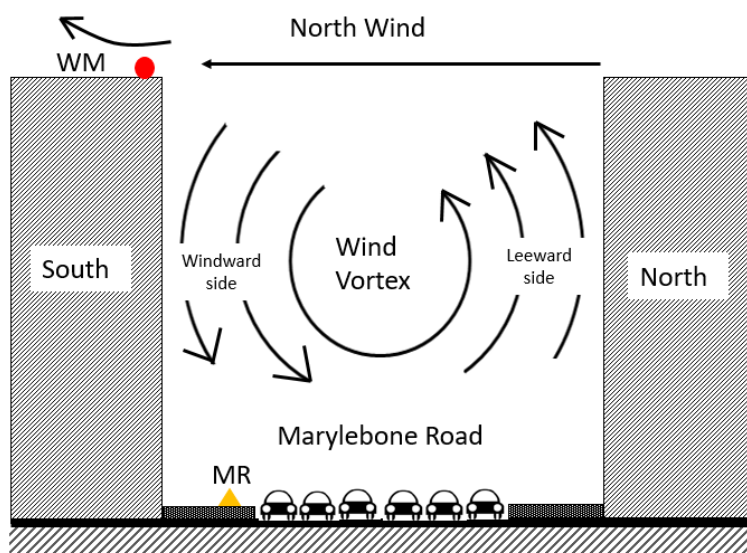
1025



1026



1027



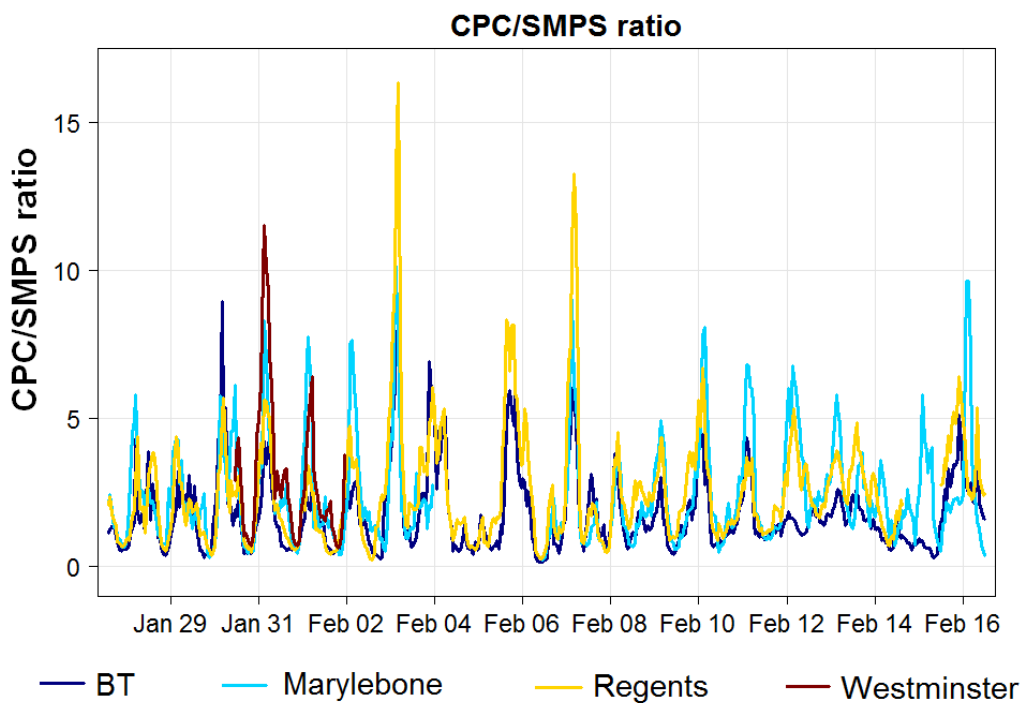
1032

Figure 6: A schematic diagram of the wind flows in the street canyon of Marylebone Road (6 traffic lanes) during southerly and northerly winds. The orange marker represents the MR sampling site and red marker represents the WM sampling site.



1033

1034



1035

1036

1037 **Figure 7:** Time series (15 min) of ratio of total particle number counts, CPC/SMPS, for four sites

1038 over the campaign period.

1039

1040

1041

1042

1043

1044

1045

1046

1047

1048

1049

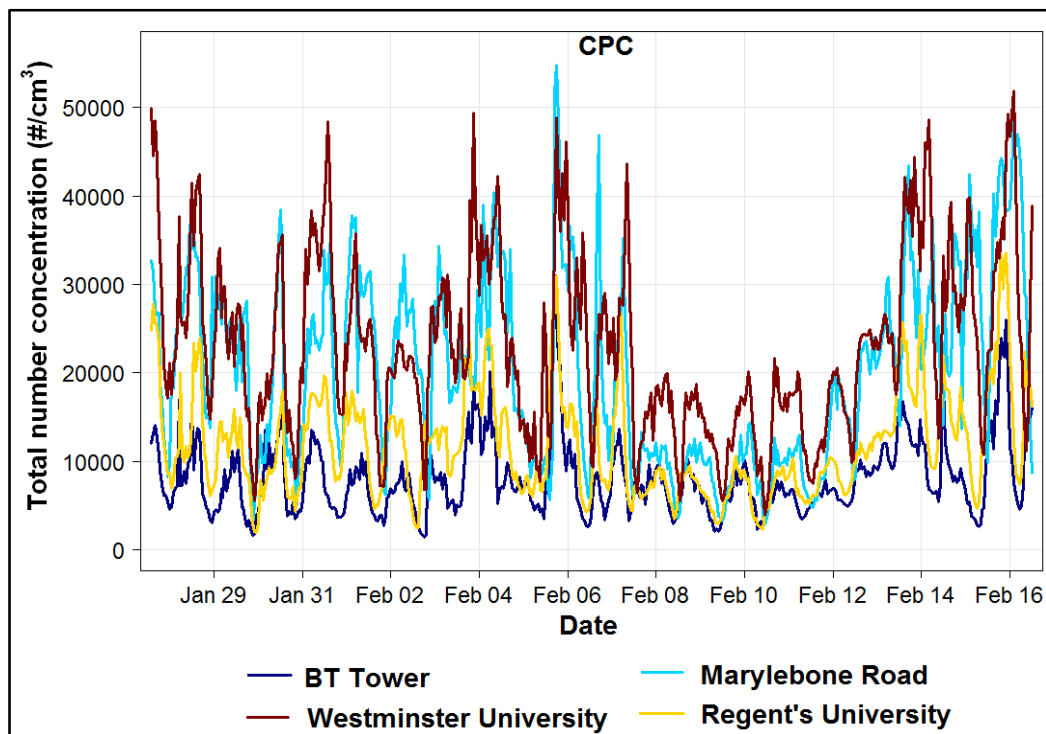
1050

1051

1052



1053



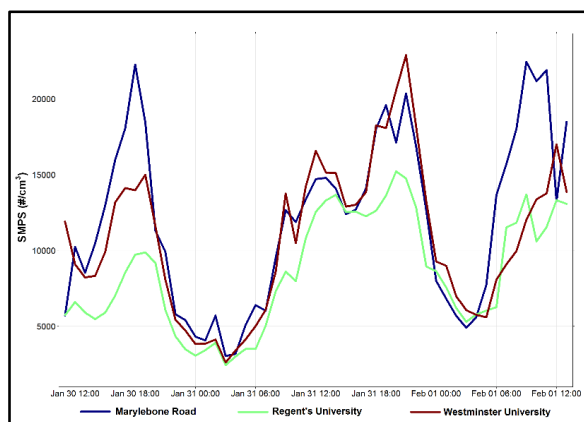
1054

1055

1056 **Figure 8:** Time series (15 min) of total particle number count from the CPC instruments located at
1057 four sites over the campaign period.

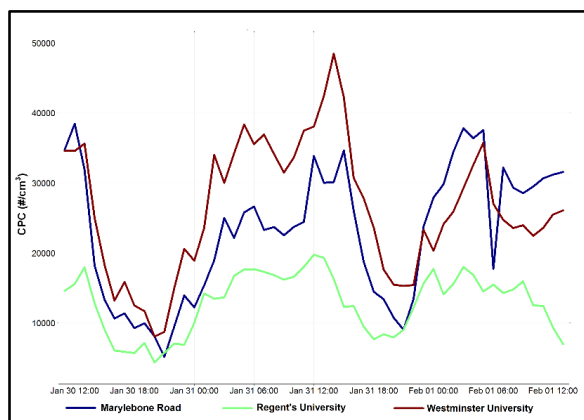
1058

1059



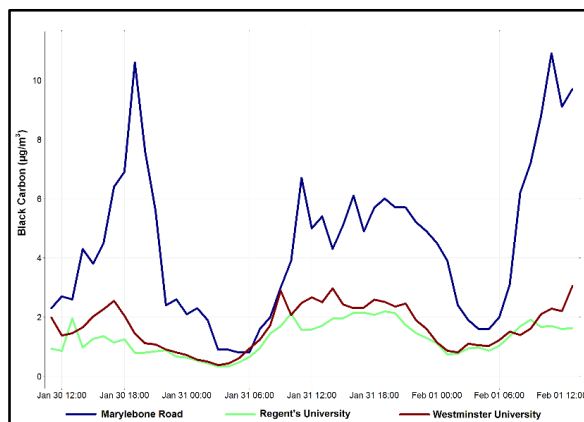
1060
(a)

1061



(b)

1063



1064
(c)

1065
1066
1067
1068
1069
1070
1071

Figure 9: Time series (15 min) of (a) SMPS integrated counts, (b) particle number counts (CPC) and (c) Black Carbon from Marylebone Road, Westminster University and Regent's University for 30 January to 1 February 2017.